



## Sensitivity Analysis of a Large-Scale Schlieren Imaging Setup When Measuring Indoor Airflow

Amayu Wakoya Gena, Lia Becher, Conrad Voelker

Department of Building Physics, Bauhaus-University Weimar, Coudraystrasse 11a, Germany

amayu.wakoya.gena@uni-weimar.de

### Abstract

In this study, the parameters of the large-scale schlieren setup at Bauhaus-University Weimar was analyzed and its sensitivity was determined. For the analysis of the sensitivity, convective indoor airflow measurements were used. Accordingly, the minimum detectable density gradient of the schlieren setup was calculated. Similarly, the setups output (schlieren image illuminance, background illuminance, and illuminance gain due to refraction) were quantified. Finally, the setups sensitivity was mathematically determined as the rate of change of schlieren output contrast with respect to the refraction angle. Further, the relationship between schlieren cut-off, refractive index, illuminance, and contrast of schlieren image were identified.

### Introduction

The schlieren imaging setup at Bauhaus-University Weimar is called a single-mirror coincident schlieren setup because it uses a single concave spherical mirror (Figure 1, Figure 3) (Gena et al., 2020). In addition, the illumination light beam from the light source and the reflected light beam (source image) from the mirror are essentially coincident. The setup consists of five elements: concave spherical mirror, LED light source (including condenser lens and pinhole), beamsplitter, schlieren cutoff, and digital camera. Figure 1 shows the diagram of single-mirror

coincident schlieren imaging system. In this setup, the LED light source is placed along the axis of the beamsplitter. It is positioned at the same distance as the radius of curvature of the spherical mirror ( $R = 2f$ ). The diverging light beam from the source passes through the beamsplitter and pinhole. Then, it fills the mirror and returns along the coincident path crossing the test object  $S$  at  $g$  distance from the mirror. The light beams get refracted by  $\Delta\varepsilon$  as it pass through the test area due to the density difference between the test subject and the surrounding air. The light beams experience vertical refractive index gradient ( $dn/dy$ ) or horizontal refractive index gradient ( $dn/dx$ ). The light beams experienced  $dn/dy$ , get refracted by  $y$ -component angle of refraction  $\Delta\varepsilon_y$ . Similarly, by  $x$ -component angle of refraction  $\Delta\varepsilon_x$  in the case of  $dn/dx$  (Settles, 2001). As a result of this refraction, these light beams do not end up at the focal point. These light beams are partially blocked at the schlieren cutoff plane. Usually, vertical schlieren cutoff is used to block the refracted light beams due to  $dn/dx$  and horizontal schlieren cutoff is used in the case of  $dn/dy$ . The blocked light beams create shadows on the schlieren image while the unblocked once brighten. Therefore, the density gradient and hence the convective air flow of the test subject will become visible on the camera screen (Settles & Hargather, 2017).

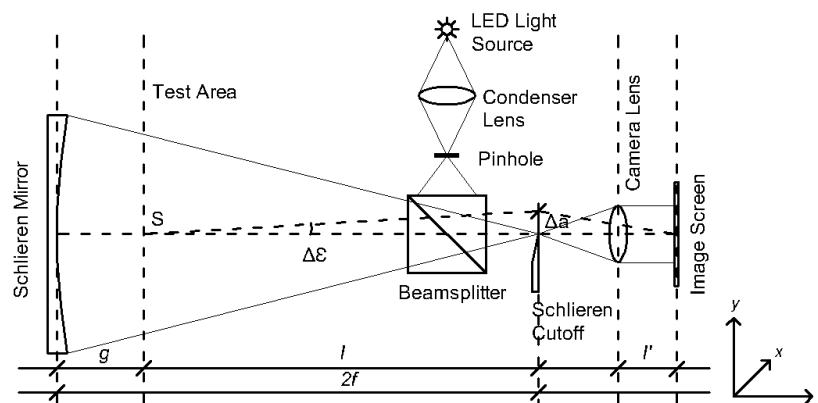


Figure 1: Diagram of the schlieren imaging setup

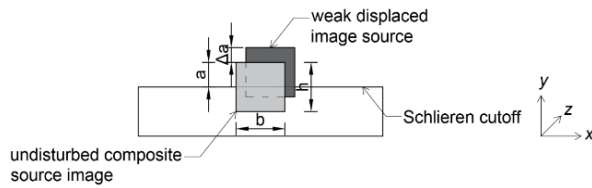


Figure 2: Horizontal schlieren cutoff plane

Further, Figure 2 illustrates horizontal schlieren cutoff orientation. The returning light rays ( $b \times h$ ) is partial blocked by schlieren cutoff. Thus, only the unblocked light beams with a height  $a$  from the total height  $h$  of LED will pass to the camera lens. Additionally, due to refraction at a point in the test area, the source image will be shifted by  $\Delta a$ .

## Measurements

### Schlieren Optical Elements

Most of the optical elements of the setup are new and have replaced the optical elements used at early stage development of the schlieren setup (Gena et al., 2020, Gena & Voelker, 2018). These optical elements were installed after multiple test, careful investigations, and literature reviews. As a result, the best fit parameters of some of the optical elements are known and optimized prior to their installation. The specifications of the elements are discussed in the following chapter.

#### Concave Spherical Schlieren Mirror

The schlieren mirror is the main optical element of the setup (Figure 3). It is made from Astrosital glass-ceramic with a 2.7 nm RMS micro-roughness and a scratch/dig surface quality of 100/80. It has the surface accuracy of  $\lambda/9.5$ , where  $\lambda$  is the wavelength of HeNe laser light. Hence, the quality of the mirror is considered as astronomical. The mirror is 1m in diameter and has a focal length of  $\approx 3$ m, making it one of the largest schlieren mirrors in the world. The mirror is strap-mounted on an adjustable carriage. Thus, it can be easily repositioned and adjusted according to the space in the lab and the test subject. In addition, the height of the mirror can be adjusted,

with the maximum height about 2m from the floor and the minimum about 0.55m.

#### LED Light Source

After preliminary tests of different light sources, the Nichia LED was selected for the setup (Figure 4). The LED is only 2.1 x 2.1 x 0.27mm in size. It has a power of 2.1W, 284lm luminous flux, 22.6 candelas of luminous intensity, and 5000K color temperature. The LED is connected to 700mA constant current supply (RACD06), as a result it forwards 2.9V or around 2W of power. The LED is placed behind a Thorlabs square pinhole  $1000 \pm 10 \mu\text{m}$  (Figure 4). Thus, the size of the point light source is defined. The LED is mounted on a 25mm Thorlabs linear XYZ translation stages with a 500  $\mu\text{m}/\text{rev}$  manual adjuster. Therefore, optical alignment at micrometer level can be achieved.

#### Beamsplitter

Since, the illumination light and reflected light beam (source image) from the mirror are essentially coincident, it can only be separated using beamsplitter. For this reason, a 30mm cage cube-mounted Thorlabs non-polarizing beamsplitter was selected (Figure 4). The beamsplitter has broadband AR-Coated faces for 400-700nm light wavelength and has 50:50 split ratio. Similarly, it is mounted on 25mm Thorlabs linear XYZ translation stages with 500  $\mu\text{m}/\text{rev}$  side-mounted micrometers for fine adjustment.

#### Schlieren Cutoff

Usually the schlieren cutoff is an ordinary razor blade. However, for maximum flexibility, different cutting percentage, and orientations (vertical or horizontal), the OWIS SP40, 7mm x7mm adjustable slit with 0.5mm/rev spindle pitch was selected as schlieren cutoff (Figure 4). The OWIS SP40 is mounted on Thorlabs linear XYZ translation stages with 500  $\mu\text{m}/\text{rev}$ . Thus, up to 10% of the pinhole size (10  $\mu\text{m}$ ) schlieren cutoff can be applied. This adjustment resolution is important for the analysis of the sensitivity of the setup.



Figure 3: The schlieren lab at Bauhaus-University Weimar

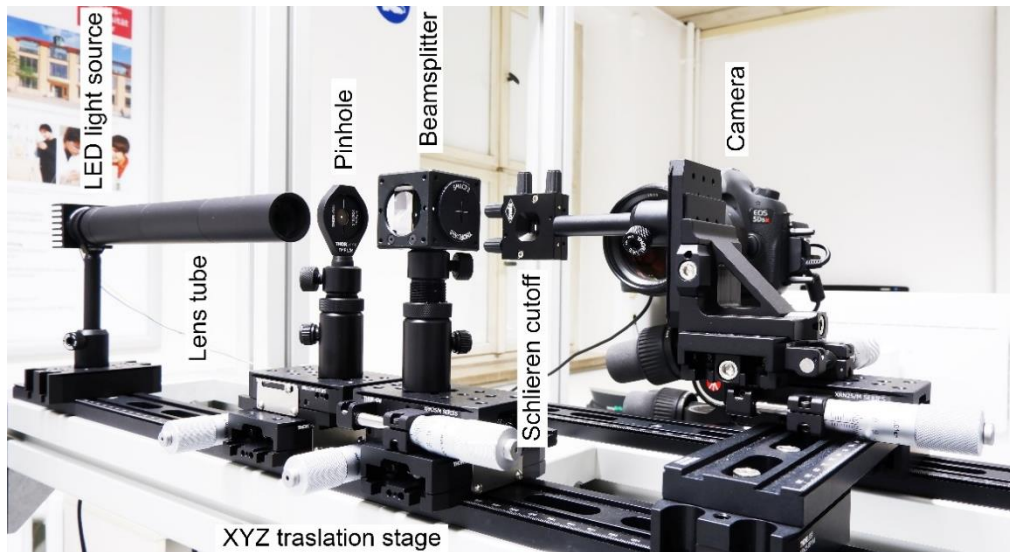


Figure 4: Optical element of the schlieren imaging setup

### Camera and Lens

The quality of schlieren images is also determined by the specifications and settings of the camera and the lens that is attached to it. The resolution and exposure time of the camera, and the aperture and the focal length of the lens are the main parameters that should be identified ahead of schlieren measurements. Considering the specifications mentioned above and the radius of curvature ( $2f \approx 6m$ ) of the schlieren mirror and the other optical elements of the setup, Canon EOS 5DSR camera and ZEISS Milvus 2/135 lens were selected (Figure 4). The camera is a digital single flex camera featuring a full frame CMOS sensor (36mm x 24mm) with 50.6 megapixels. It has a mechanical shutter speed has a minimum of 1/8000 seconds and maximum of 30 seconds. Therefore, with the minimum exposure time, it is possible to capture the structures of indoor air gradients. The camera has an ISO range between 100 to 6400 in 1/3-stop increments. The lowest ISO is preferred for the reduction of the amount of noise on the schlieren image. The lens has 135mm focal length, with focusing range from 0.80m to infinite. The aperture of the lens ranges between  $f/2$  and  $f/22$ . Usually, schlieren measurements take place in the room with no light other than the setups light source, thus the wider aperture  $f/2$  is recommended as it allows more light to pass to the camera sensor.

### **Schlieren measurements**

Sensitivity of a measuring instrument can be defined as the relationship between the instrument's output and the input received (Settles, 2001). In case of schlieren measurements, sensitivity is the relationship between the schlieren output (e.g. 2D image contrast) and the input (deflected rays due to refractive-index gradients in the airflow). Identifying this relationship helps to

understand the connection between the schlieren elements and their parameters. Additionally, it can be used to classify the optimal settings of the setup. Therefore, the minimum density gradient can be detected. To estimate this minimum density gradient, the analysis of indoor airflow measurements was carried out. For this reason, a laminar flow analysis was preferred. To generate a laminar flow, a 5mm thick heated copper plate (190mm x 190mm) was used. The plate was heated overnight in heating and drying oven at 40°C. After uniform surface temperature was achieved, the plate was carefully placed in front of schlieren mirror (Figure 5).

To measure the air temperature above the heated plate, four Ahlborn's negative-temperature-coefficient thermistors (NTC) with an accuracy of  $\pm 0.1K$  were used. The NTCs were placed with 50mm gap above the plate along the stream of the flow (Figure 5). The measurements were carried out for 15 minutes with 1 second interval. Simultaneously, the room air temperature was measured. It was nearly constant (around 21.24°C) as there is no other heat source in the room other than the plate and the author who was seating far from test area behind the camera. Similarly, the room air velocity was nearly zero. The velocity was measured using an Ahlborn hot-wire omnidirectional anemometers with  $\pm 1.5\%$  accuracy. During the schlieren measurements 50% schlieren cutoff was used.



Figure 5 Schlieren visualization of convective thermal plume above hot copper plate and positioning of NTC sensors (black dots, dimension is in mm)

## Results and Discussions

To determine the sensitivity of the setup, luminance and refractive analysis of the schlieren measurements were conducted. For these analyses, some of the optical elements parameters and settings were considered as predefined constraints. Thus, the parameters of other optical elements can be improved based on these constraints. Some of the known constraints are: the camera aperture ( $f/2$ ), the lowest ISO number (ISO 100), and maximum luminance emitted by the light source ( $5.12 \times 10^6 \text{ candela/m}^2$ ).

### Luminance Analysis

In schlieren imaging, luminance is used to quantify the amount of light passing through the test area. Furthermore, it is used to determine the schlieren image illuminance. In the presence of schlieren cutoff, the luminance of the light source can also be used to calculate the background illuminance of schlieren image. This background illuminance is dependent of the percentage of schlieren cutoff. To calculate these illuminances, the geometrical optics of the setup is used (Figure 1). By definition, luminance is an intensity per unit area. Therefore, the luminance  $B$  of the LED light source is,

$$B = \frac{\text{luminous flux (candelas)}}{h_{LED} \cdot b_{LED} (m^2)} \quad (1)$$

$$B = 5.12 \times 10^6 \text{ candela/m}^2$$

Further, by way of the inverse square law, illuminance incident up on the schlieren mirror  $E_m$  can be estimated. Thus, from Figure 1 and 2,

$$E_m = \frac{B \cdot b_{pinhole} \cdot h_{pinhole}}{f^2} \quad (2)$$

$b_{pinhole}$  and  $h_{pinhole}$  = the breadth and height of the pinhole;  $f$  = the distance between the light source and the schlieren mirror. Since the area of the LED ( $4.41 \text{ mm}^2$ ) is bigger than the pinhole ( $1 \text{ mm}^2$ ), the luminance of the light sources decreases by around 77% as it passes through the pinhole. Thus, after the pinhole, the luminance of the LED  $B$  would be

$1.16 \times 10^6 \text{ candela/m}^2$ . In addition, because of the 50:50 beamsplitter, the luminance is reduced by half. Thus,  $E_m = 1.61 \times 10^{-2} \text{ lux}$ . However, on the way back from the mirror, the light beam passes through the beamsplitter once more. At the absence of the schlieren cutoff, the illuminance of the schlieren image illuminance  $E_o$  will be quarter of  $B$ . A magnification factor  $m$  should be considered for image size relative to that of the test area when calculating  $E_o$ . In this case the standard thin-lens-formula can be used to determine the schlieren image magnification factor (Settles, 2001). Thus, schlieren image magnification factor  $m = 2.5\%$  was calculated. Hence, the schlieren image illuminance  $E_o$  is,

$$E_o = \frac{B \cdot b_{pinhole} \cdot h_{pinhole}}{m^2 f^2} \quad (3)$$

$$E_o = 0.13 \times 10^2 \text{ lux}$$

According to Equation (3),  $E_o$  is schlieren image illuminance without schlieren cutoff. However, when schlieren cutoff advances, the background and overall illuminance of schlieren image changes. The background illuminance of schlieren image  $E_b$  can be estimated by replacing  $h_{pinhole}$  in Equation (3) by  $a$  to represent the actual height of the light source image after the schlieren cutoff.

$$E_b = \frac{\frac{1}{4} B \cdot b_{pinhole} \cdot a}{m^2 f^2} \quad (4)$$

Finally, using Equation (4) the background illuminance of schlieren image  $E_b$  was estimated for different percentage of the schlieren cutoff (Figure 6).

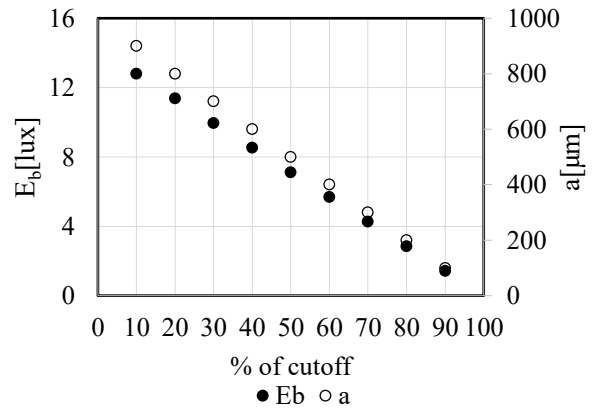


Figure 6: Background illuminance ( $E_b$ )

Figure 6 shows, when 10% ( $a = 100 \mu\text{m}$ ) schlieren cutoff advances, the background illuminance of schlieren image changes by  $\Delta E_b = 0.012 \times 10^2 \text{ lux}$ . This change in illuminance  $\Delta E$  results an overall change on schlieren image contrast. Consequently, the contrast of schlieren image can be referred as the ratio of differential illuminance  $\Delta E$  at the image point to the general background level  $E_b$  (Equation 5).

$$C = \frac{\Delta E}{E_b} \quad (5)$$

This image contrast  $C$  is the output of schlieren measurement with the input being a pattern of irregular ray deflections resulting from refractive-index gradients in the test area. Since the sensitivity of any instrument is basically the ratio of change in the output  $d(output)$  and input  $d(input)$ , thus the sensitivity of the schlieren setup is the rate of change of image contrast  $C$  with respect to refraction angle  $\Delta\epsilon$  (Equation 6). The details are discussed below.

$$S = \frac{dC}{d\epsilon} \quad (6)$$

### Refractive Analysis

Schlieren imaging capitalizes the refraction of light. This refraction due to density difference can be quantified, and used to determine the sensitivity of the schlieren setup. The following steps were used to quantify the refraction. Firstly, measurements of air temperature  $T$  and local pressure  $P$  were conducted.  $P$  can also be derived from atmospheric data and the local height above sea level. Secondly, calculate air density  $\rho$  using perfect gas state equation (Equation 7).

$$\rho = \frac{P}{RT} \quad (7)$$

$R$  = the specific gas constant at 1 bar air pressure ( $R = 287.058 \text{ Pa} \times \text{m}^3/\text{kg}$ ).

Once the air density  $\rho$  is calculated, using the Gladstone-Dale relation (Equation 8) the refractive index  $n$  can be evaluated.

$$n - 1 = k\rho \quad (8)$$

$k$  = the Gladstone-Dale coefficient ( $k \approx 2.30 \times 10^{-4} \text{ m}^3/\text{kg}$ ) for air at standard conditions.

Based on Equation (7) and (8) both refractive index of the thermal plume above the hot plate at 0.05m, 0.1m, 0.15m, and 0.2m and the room air can be calculated. As a result, the refractive index of the test object  $n_{plume}$  and the surrounding air  $n_{room\ air}$  can be calculated (Figure 7). However, to determine the sensitivity of the setup, the refraction angle  $\Delta\epsilon$  must be known (Figure 1). In this case, thin-lens approximation of geometrical optics (Equation 9) was used to approximate the refraction angle  $\Delta\epsilon$  (Settles, 2001)

$$\Delta\epsilon = 2\left(\frac{n_{plume}}{n_{room\ air}} - 1\right) \quad (9)$$

Accordingly, the refraction angles  $\Delta\epsilon$  at 0.05m, 0.1m, 0.15m, and 0.2m above the hot plate were calculated (Figure 7).

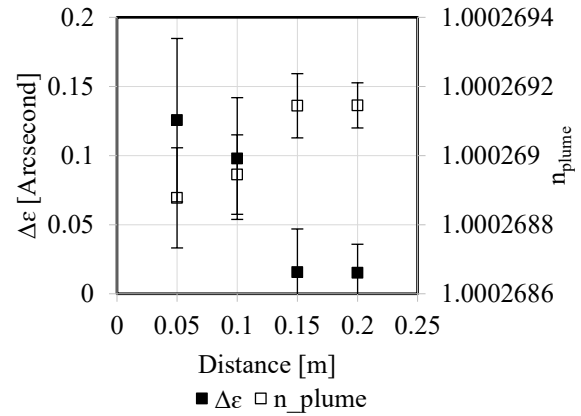


Figure 7. The refraction angles and refractive index of the test object at corresponding points

Figure 7 shows that, the maximum  $\Delta\epsilon$  is at 0.05m above the hot copper plate, measuring slightly above 0.1arcseconds. The refraction angle  $\Delta\epsilon$  at 0.15m and 0.2m are comparable. At both locations,  $\Delta\epsilon$  is less than 0.05arcseconds. These shows,  $\Delta\epsilon$  decreases as the distance from the coper plate increases. Which is due to temperature reduction with height. The figure also shows, the inverse relationship between  $\Delta\epsilon$  and refractive index ( $n_{plume}$ ). The error bar indicates the range of  $\Delta\epsilon$  and  $n_{plume}$  for the NTC measurements duration. Relatively a bigger interval of error bar is observed at 0.05m. This could be due to the fact that at this height the flow is relatively turbulent, thus affects the NTC sensors measurements. Similar instance was observed on Figure 8 and Figure 9.

In addition, using the geometric optics of the setup, the shifts of the source image  $\Delta a$  due to  $\Delta\epsilon$  can be derived (Equation 10). As a result,  $\Delta a$  at corresponding points at 0.05m, 0.1m, 0.15m, and 0.2m were calculated (Figure 8).

$$\Delta a = \tan \Delta\epsilon \times l \quad (10)$$

Further,  $\Delta a$  can substitute  $a$  in Equation (4), thus to determine the additional gain of illuminance  $\Delta E$  due to  $\Delta\epsilon$  in the test area (Equation 11).

$$\Delta E = \frac{1}{4} \frac{B \cdot b \cdot \Delta a}{m^2 f} \quad (11)$$

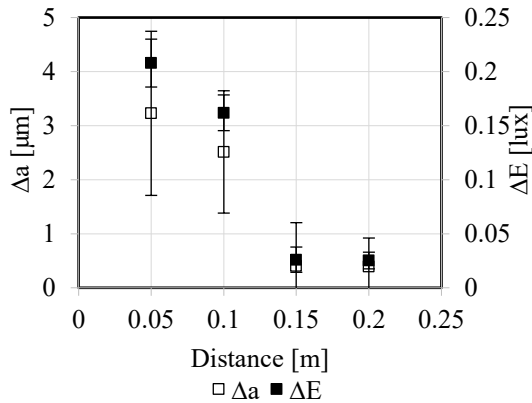


Figure 8. The incremental gain of illuminance  $\Delta E$  due to the  $\Delta a$  at the corresponding image points

Figure 8 shows, the shift of the source image  $\Delta a$  at schlieren cutoff due of  $\Delta \epsilon$  is less than  $1 \mu\text{m}$ . This result shows the micrometer resolution of the setup, hence emphasizes the high sensitivity of the setup and its application for indoor climate studies. In addition, the figure shows,  $\Delta a$  has liner relationship with  $\Delta E$ . It also underlines the bigger  $\Delta a$  the higher illuminance of schlieren image.

Finally, using Equation (5) and (6), the contrast  $C$  and sensitivity  $S$  of the setup were estimated (Figure 9). Figure 9 shows, for 50% of schlieren cutoff, the contrast of the schlieren measurements are below 4%. Which is weak but clearly visible (Figure 5). Also, equation (6) yields a sensitivity around 70% contrast change per arcsecond of refraction.

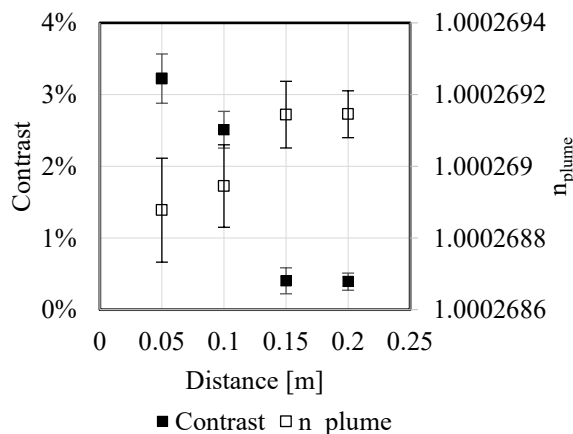


Figure 9. Contrast of the schlieren image points in relation to the refractive index

## Conclusion

The findings of this study show that the minimum detectable density gradient of the schlieren setup at Bauhaus-University Weimar. The results also illustrate the mathematical approach used to quantify the output of schlieren measurements. Consequently, the setups sensitivity, schlieren image contrast, illumination, refraction angles, and the shift of the source image due to refraction angles were calculated.

Further, the correlation between schlieren cut-off, refractive index, illuminance, and contrast of schlieren image were identified.

All these findings demonstrate the schlieren setup is capable of imagining indoor density gradient as small as 0.05arcseconds of refraction. The results also emphasize the setup is capable of clearly visualizing flow features with only 4% of image contrast. Thus, the setup yields a sensitivity around 70% contrast change per arcsecond of refraction.

## Acknowledgement

The authors are grateful to the German Research Foundation DFG (Grant no. 444059583) for funding this project. Their support is highly appreciated.

## References

- Gena AW, Völker C. 2018. Setup, measurements and first results of a new schlieren imaging system. Proceedings of ISFV18, Zürich, Switzerland.
- Gena AW, Voelker C, Settles GS. 2020. Qualitative and quantitative schlieren optical measurement of the human thermal plume. Indoor Air.
- Settles GS, Hargather MJ. 2017. A review of recent developments in schlieren and shadowgraph techniques. Measurement Science and Technology.
- Settles G. Schlieren and shadowgraph techniques. 2001. Heidelberg, Germany.